

Anti-screening of the Galileon force around a disk center hole

Hiromu Ogawa,^{1,2,*} Takashi Hiramatsu,^{1,†} and Tsutomu Kobayashi^{1,‡}

¹*Department of Physics, Rikkyo University, Toshima, Tokyo 171-8501, Japan*

²*Institute of Cosmology and Gravitation, University of Portsmouth, Portsmouth, PO1 3FX, UK*

The Vainshtein mechanism is known as an efficient way of screening the fifth force around a matter source in modified gravity. This has been verified mainly in highly symmetric matter configurations. To study how the Vainshtein mechanism works in a less symmetric setup, we numerically solve the scalar field equation around a disk with a hole at its center in the cubic Galileon theory. We find, surprisingly, that the Galileon force is enhanced, rather than suppressed, in the vicinity of the hole. This anti-screening effect is larger for a thinner, less massive disk with a smaller hole. At this stage our setup is only of academic interest and its astrophysical consequences are unclear, but this result implies that the Vainshtein screening mechanism around less symmetric matter configurations is quite nontrivial.

PACS numbers: 04.50.Kd

arXiv:1802.04969v1 [gr-qc] 14 Feb 2018

* Email: jh.ogawa@rikkyo.ac.jp

† Email: hiramat@rikkyo.ac.jp

‡ Email: tsutomu@rikkyo.ac.jp

I. INTRODUCTION

The origin of the current accelerated expansion of the Universe [1, 2] is one of the biggest problem in modern physics (see [3–6] for several independent observations). In order to explain this phenomenon, one basically has to introduce an unknown energy source, i.e., dark energy [7]. The simplest possibility is the cosmological constant, and introducing another unknown component, i.e., dark matter, the Λ CDM model is well compatible with observations. This concordance model, however, suffers from the fine-tuning problem of the cosmological constant. The mystery of the accelerated expansion of the Universe thus motivates us to explore the possibilities of modification of general relativity on cosmological scales [8].

A number of theories have been proposed so far as alternatives to the cosmological constant and dark energy. Most of them can be described (effectively) by a scalar-tensor theory, which has a scalar degree of freedom in addition to the two tensor modes. This scalar mediates a new long-range force, i.e., a fifth force. Since any deviation from general relativity is strongly constrained in the solar system [9, 10], scalar-tensor theories must possess a mechanism for screening the fifth force in the vicinity of matter sources such as in the solar system.

Several types of screening mechanisms have been known so far. The first one relies on the potential term of the scalar degree of freedom. The shape of the potential is designed so that the scalar becomes effectively massive in a high density region. This class of models include chameleon [11], symmetron [12], and dilaton [13] mechanisms. The second one relies on nonlinear derivative interactions of the scalar field, by which the kinetic term of the scalar becomes effectively large and hence it is effectively weakly coupled to matter near the source where its gradient is large. This class can be divided into two subclasses depending on whether first or second derivatives of the scalar field play a crucial role. The former includes models of [14–16] and the latter includes the Galileons [17–19]. The screening mechanism in this last class of models is called the Vainshtein mechanism [20], and has been studied extensively (see Ref. [21] for a review). The Vainshtein mechanism has been investigated [22–25] even in the context of the most general scalar-tensor theory with second-order field equations [26] because it can be obtained by generalizing the Galileons [27, 28] and the mechanism can thus be implemented naturally. See Refs. [29–32] for the Vainshtein mechanism (and its partial breaking) in more general scalar-tensor theories which have been developed recently.

Previous works mostly focused on the Vainshtein mechanism around spherical distributions of matter, as a star can be well approximated by a sphere. The authors of [33] have investigated analytically the systems with cylindrical and planar symmetries, and found that screening is weaker in the cylindrically symmetric case and does not occur in the system with planar symmetry. This implies that Vainshtein screening might be sensitive to the shape of the matter distribution. It is, however, difficult in general to study the shape dependence of the Vainshtein mechanism because one has to treat derivative nonlinearities in less symmetric systems. In Ref. [34], a two-body system was investigated numerically and it was shown that the equivalence principle can be violated apparently in such systems. Approximate solutions for slowly rotating stars in the cubic Galileon theory were obtained in Ref. [35]. As for a dynamical aspect of the Vainshtein mechanism, the emission of scalar modes from a binary system was evaluated in Ref. [36]. Very recently the shape dependence of screening in the chameleon theory was addressed numerically in Ref. [37].

In this paper, we consider a disk with a hole at its center as a source and solve the Galileon field equation fully numerically in order to address the consequence of nonlinear derivative interactions in a less symmetric system. We only study the cubic Galileons for simplicity. A similar system in a different theory of modified gravity has been considered in Refs. [38, 39], where scalar field profiles around a black hole accretion disk have been investigated in the context of the chameleon theory.

The outline of this paper is as follows. In the next section, we summarize briefly the cubic Galileon theory and describe our numerical setup. We then present our main results in Sec. III. Finally, we draw our conclusions in Sec. IV. In the main text we only consider the Galileon field living in a flat background. To see how our result depends on the background curvature, in Appendix A we give a numerical result in the fixed Schwarzschild background. Details of the numerical scheme are given in Appendix B.

II. BASIC EQUATIONS

A. The cubic Galileon

We consider the cubic Galileon theory [17, 18] as an example of the model endowed with the Vainshtein mechanism. In the Einstein frame, the cubic Galileon ϕ and its coupling to matter are described by the action

$$S = \int d^4x \left[-\frac{1}{2}(\partial\phi)^2 - \frac{c_3}{M^3}(\partial\phi)^2\Box\phi + \frac{\beta}{M_{\text{Pl}}}\phi T^\mu{}_\mu \right], \quad (1)$$

where c_3 and β are dimensionless parameters, M_{Pl} is the Planck mass, M is another mass scale, and T_μ^μ is the trace of the matter energy-momentum tensor. We assume that matter is non-relativistic, so that $T_\mu^\mu \simeq -\rho$. Varying the action with respect to ϕ , we obtain the field equation,

$$\Delta\phi + \frac{c_3}{M^3} [(\Delta\phi)^2 - \nabla_i \nabla_j \phi \nabla^i \nabla^j \phi] = \frac{\beta}{M_{\text{Pl}}} \rho, \quad (2)$$

where we assumed that ϕ is static. For a given configuration of matter, one can integrate Eq. (2) to obtain the profile of ϕ .

The coupling between matter and the metric fluctuations around the Minkowski spacetime, $h_{\mu\nu}$, is expressed as $(1/2)h_{\mu\nu}T^{\mu\nu}$. This implies that the Jordan frame metric is given by $h_{\mu\nu}^{\text{J}} = h_{\mu\nu} + (2\beta/M_{\text{Pl}})\phi\eta_{\mu\nu}$, and thus a test particle of mass m feels the fifth force

$$\vec{F}_\phi = -\frac{\beta}{M_{\text{Pl}}} m \vec{\nabla}\phi, \quad (3)$$

in addition to the usual gravitational force $\vec{F}_{\text{grav}} = (m/2)\vec{\nabla}h_{00}$.

Let us consider the profile of ϕ around a spherical matter configuration. In this case, using the spherical coordinates it is easy to get

$$\vec{\nabla}\phi = \frac{M^3}{4c_3} r \left(-1 + \sqrt{1 + \frac{2c_3\beta}{\pi M^3 M_{\text{Pl}}} \frac{\mathcal{M}}{r^3}} \right) \vec{e}_r, \quad (4)$$

where \vec{e}_r is the radial unit vector and \mathcal{M} is the mass of the spherical body. For $r \gg r_V := (2c_3\beta\mathcal{M}/\pi M^3 M_{\text{Pl}})^{1/3}$, we have $|\vec{F}_\phi| = \mathcal{O}(\beta^2|\vec{F}_{\text{grav}}|)$, implying that the fifth force is as large as the usual gravitational force if $\beta = \mathcal{O}(1)$. However, for $r \ll r_V$ we find that $|\vec{F}_\phi| = (r/r_V)^{3/2} \mathcal{O}(\beta^2|\vec{F}_{\text{grav}}|) \ll \mathcal{O}(|\vec{F}_{\text{grav}}|)$, and thus the fifth force is screened in the vicinity of the body. This is the Vainshtein mechanism. For this to happen the non-linear term in Eq. (2) plays a crucial role. In order to pass laboratory and solar-system tests of gravity, M^3/c_3 must be sufficiently small so that r_V is sufficiently large.

So far, successful Vainshtein screening has been confirmed mainly for spherically symmetric configurations. The Vainshtein mechanism in the systems with planar and cylindrical symmetry has been investigated in Ref. [33], and it was found that the screening of the fifth force is sensitive to the shape of the matter distribution. Only in such highly symmetric cases the non-linear equation (2) can be integrated analytically, and one has to employ numerical methods in general cases. In Ref. [34] the Galileon field equation is integrated numerically for a two-body system. In the present paper, we examine the profile of the Galileon field around a matter distribution that has not been investigated previously, i.e., a disk with a hole.

B. Numerical setup

Specifically, we model the system by the following uniform density profile

$$\rho(r, \theta) = \rho_0 U(r - r_1) U(r_2 - r) U(\theta_0 - \theta) U(\theta_0 + \theta), \quad (5)$$

$$\rho_0 = \text{const}, \quad (6)$$

where U is the Heaviside function, with r_1 , r_2 , and θ_0 being the inner radius, the outer radius, and the (half of the) opening angle of the disk, respectively (Fig. 1). Note that here we are using the spherical coordinates whose definition is slightly different from the usual one, $x = r \cos \theta \cos \varphi$, $y = r \cos \theta \sin \varphi$, $z = r \sin \theta$, with $-\pi/2 \leq \theta \leq \pi/2$.

To implement numerical integration, we introduce the following dimensionless quantities:

$$\bar{\phi} := \frac{\phi}{M^3 r_0^2}, \quad \bar{r} := \frac{r}{r_0}, \quad \mu := \frac{\beta \rho_0}{M^3 M_{\text{Pl}}}, \quad (7)$$

where r_0 is some arbitrary length scale and μ is the parameter that corresponds to the coupling between matter and the Galileon for fixed ρ_0 . At a sufficiently large distance from the disk object, it can be regarded as a point particle and hence we have $\bar{\phi} \sim \mu/\bar{r}^2$. Therefore, it can be said that μ controls the nonlinearity of the scalar field. We rewrite Eq. (2) in terms of the above variables assuming that ϕ is axisymmetric.

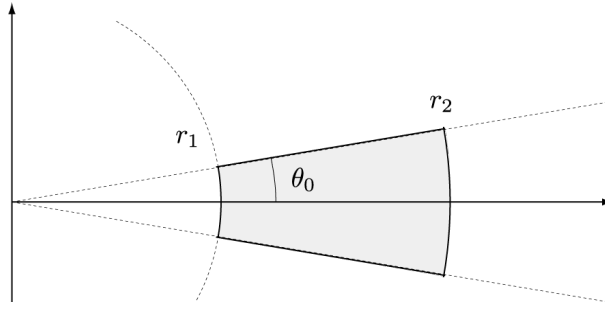


FIG. 1. A disk object with a hole in spherical coordinates.

The boundary conditions we impose are given by

$$\left. \frac{\partial \bar{\phi}}{\partial \bar{r}} \right|_{\bar{r}=0} = 0, \quad (8)$$

$$\left. \frac{\partial \bar{\phi}}{\partial \theta} \right|_{\theta=0} = \left. \frac{\partial \bar{\phi}}{\partial \theta} \right|_{\theta=\pi/2} = 0, \quad (9)$$

$$\bar{\phi}(\bar{r}_{\max}, \theta) = 0, \quad (10)$$

where $\bar{r}_{\max} := r_{\max}/r_0$ corresponds to the boundary of the computational domain. The boundary condition (8) amounts to the regularity at the center, while the condition (9) reflects the symmetry of the system. Since the field equation is invariant under the constant shift of the scalar field, $\phi \rightarrow \phi + c$, we may impose the boundary condition (10) without loss of generality.

One may naively expect that derivative nonlinearity of the Galileon field is large for $r \lesssim (c_3 \beta \rho_0 V / M^2 M_{\text{Pl}})^{1/3}$, where V is the size of a massive object. If we roughly take $r_1 \sim r_2$, we can estimate V as $V \sim r_2^3 \theta_0$. Thus, in terms of the dimensionless variables, we see that the nonlinear effect is large for $\bar{r} \lesssim (c_3 \mu \theta_0)^{1/3} \bar{r}_2$.

III. NUMERICAL RESULTS

We now present our numerical solutions to Eq. (2). We fix \bar{r}_2 and \bar{r}_{\max} as $\bar{r}_2 = 30$ and $\bar{r}_{\max} = 80$, respectively, and performed numerical calculations for different values of r_1 , θ_0 , and μ . The number of data points is 200 in the r direction and 100 in the θ direction. The details of the numerical computation are described in the Appendix B.

In Fig. 2 we show a vector plot of the dimensionless force field $-(M^3 r_0)^{-1} \vec{\nabla} \phi$ for $c_3 = 1$, $\bar{r}_1 = 8$, $\theta_0 = 0.05$, and $\mu = 36.8$. In order to clarify the effect of the nonlinear terms in Eq. (2), we also calculated the force field with the same parameters, but with $c_3 = 0$. The result is also presented in Fig. 2 for comparison. It can be seen that in the $c_3 = 1$ case the fifth force is suppressed compared to the $c_3 = 0$ case in almost every region, as expected. This is clear in particular for $\bar{r} \gtrsim 20$ around the disk. However, surprisingly enough, the nonlinear effect *enhances*, rather than suppresses, the fifth force in the vicinity of the hole.

To quantify this anti-screening effect, we introduce the following scalar quantity,

$$\mathcal{R} = \frac{|\vec{\nabla} \phi|_{c_3=1}}{|\vec{\nabla} \phi|_{c_3=0}}. \quad (11)$$

We may say that screening is successful if $\mathcal{R} < 1$. Figure 3 shows \mathcal{R} for the above case, which clearly indicates that the fifth force is enhanced near the hole.

To see how the enhancement of the fifth force depends on the parameters, we provide numerical results for different values of r_1 , θ_0 and μ in Figs. 4–6. Figure 4 shows \mathcal{R} for different sizes of the hole, $\bar{r}_1 = 4$ and 20, with c_3 , r_1 , θ_0 being fixed to the previous values and μ being given such that the total mass of the disk is unchanged from the previous case. It is found that the fifth force around the hole is stronger for a smaller hole size, as is most clearly seen in the bottom panel of Fig. 4. Figure 5 represents the dependence of the enhancement effect on the thickness of the disk. We see that for smaller θ_0 , i.e., for a thinner disk, the fifth force around the hole is stronger. Finally, we see from Fig. 6 how increasing μ changes the result with other parameters fixed. For larger μ , the enhancement of the Galileon force is less evident. This is because larger μ implies that the disk is (effectively) more dense or more massive, and thus

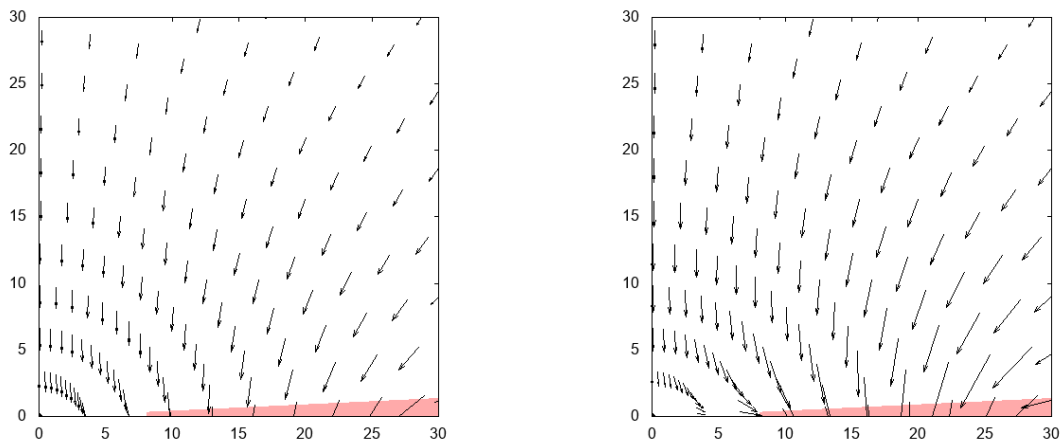


FIG. 2. Dimensionless force fields for $\bar{r}_1 = 8$, $\theta_0 = 0.05$, and $\mu = 36.8$, with $c_3 = 1$ (left) and $c_3 = 0$ (right). The thin black region represents the disk.

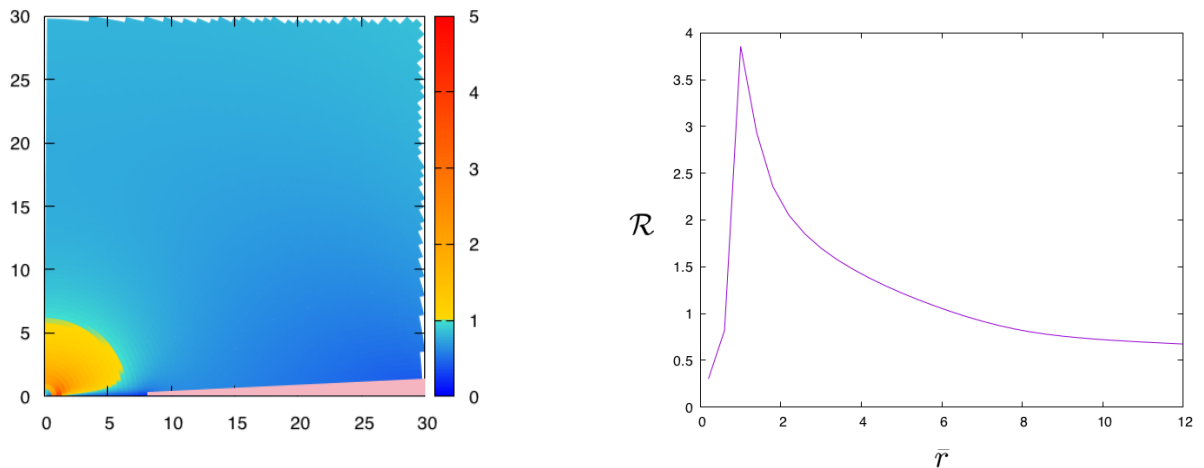


FIG. 3. 2D plot of the degree of (anti-)screening \mathcal{R} for the case shown in Fig. 2 (left) and \mathcal{R} along $\theta = 2\pi/5$ as a function of \bar{r} (right).

the screening effect from the disk itself is more efficient. To sum up, the anti-screening effect is larger for a thinner, less massive disk with a smaller hole.

IV. DISCUSSION

In this paper, we have studied numerically the fifth force around a disk with a hole at its center in the cubic Galileon theory. It is known that Vainshtein screening does not work for infinite planar sources [33]. Since our source is thin but finite, we have seen that screening still occurs in almost every region around the disk. However, we have found that the hole at the center causes an unexpected consequence: the Galileon force is not suppressed but enhanced in the vicinity of the hole, namely, anti-screening operates. Anti-screening we have seen in this paper occurs in the region where nonlinearity of the Galileon field is dominant and the configuration of matter is less symmetric. Due to this complexity, so far we have not arrived at analytic understanding of our result.

Some of the parameters we have used in our numerical calculations might not be realistic. In particular, we have seen that we need $\mu \lesssim 10^3$ in order for the force to be enhanced. For larger μ , the effect of anti-screening is washed away by the screening effect from the disk in the present setup. If the Galileon field is responsible for the current cosmic acceleration, one would expect $M^3 \sim M_{\text{Pl}} H_0^2 \sim \bar{\rho}/M_{\text{Pl}}$, where H_0 is the present Hubble parameter and $\bar{\rho}$ is

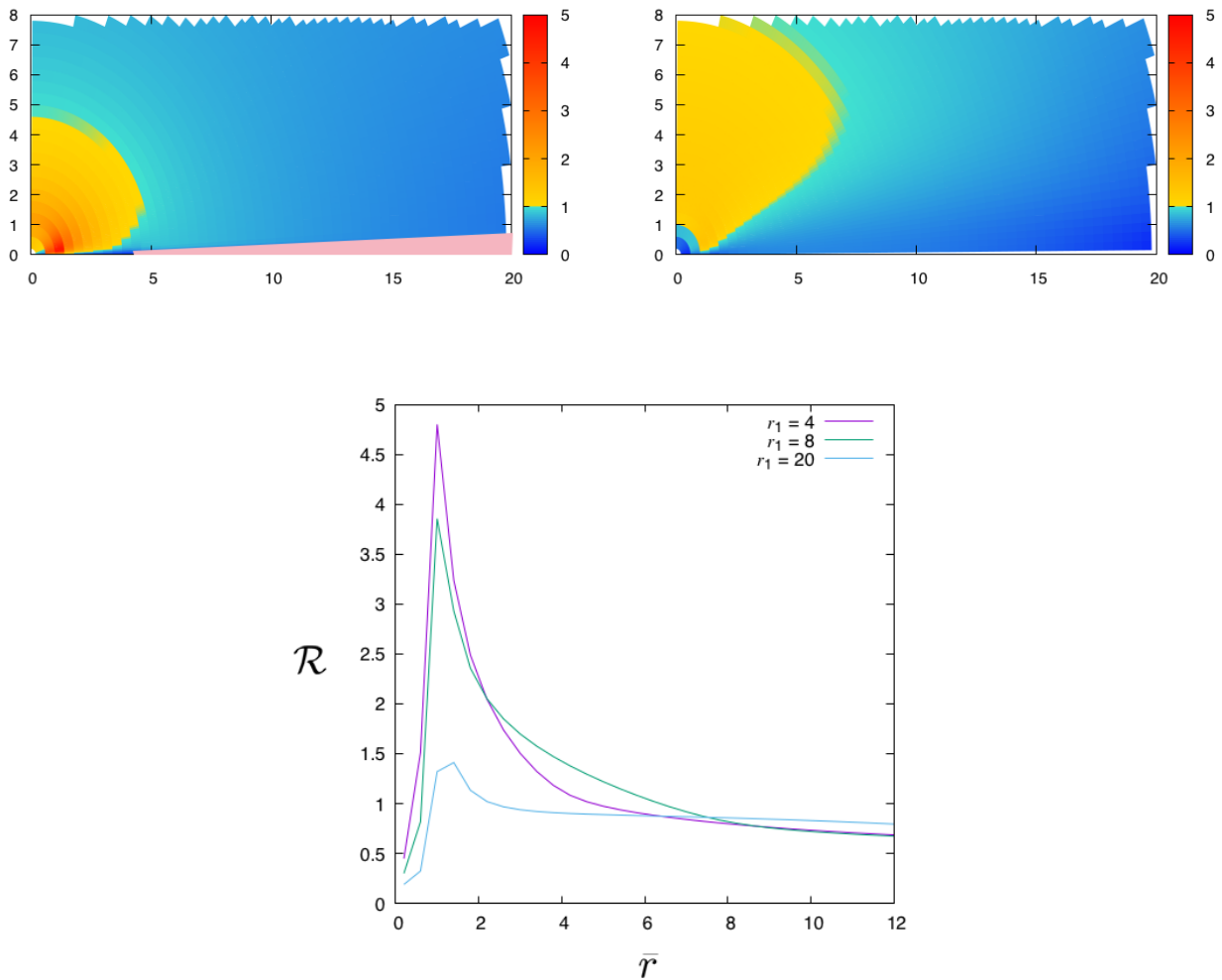


FIG. 4. \mathcal{R} for $r_1/r_0 = 4$ (top left) and $r_1/r_0 = 20$ (top right). The other parameters are the same as in the previous plots. \mathcal{R} along $\theta = 2\pi/5$ as a function of \bar{r} is also shown (bottom).

the average energy density of the Universe. The energy density of our disk is thus given by $\rho_0 \sim \mu\bar{\rho}$, assuming that $\beta = \mathcal{O}(1)$. Our numerical calculations correspond to such very low density matter distribution. Therefore, at this stage it is difficult to derive direct implications of our results for astrophysics and experiments. Nevertheless, we believe that it is interesting to further explore how the (anti-)screening mechanism operates for nontrivial configurations of matter and the present work provides a first step toward understanding this complicated problem.

ACKNOWLEDGMENTS

We thank Christos Charmousis, A. Emir Gümrukçüoğlu, Tomohiro Harada, and Kazuya Koyama for useful comments. H.O. also thanks Kazuya Koyama for his kind hospitality at University of Portsmouth where part of this work was done. This work was supported in part by the Rikkyo University Special Fund for Research (H.O.), JSPS Overseas Challenge Program for Young Researchers (H.O.), the JSPS Grants-in-Aid for Scientific Research Nos. 16K17695 (T.H.), 16H01102, and 16K17707 (T.K.), MEXT-Supported Program for the Strategic Research Foundation at Private Universities, 2014-2017 (S1411024) (T.H. and T.K.), and MEXT KAKENHI Grant Nos. 15H05888 (T.K.) and 17H06359 (T.K.).

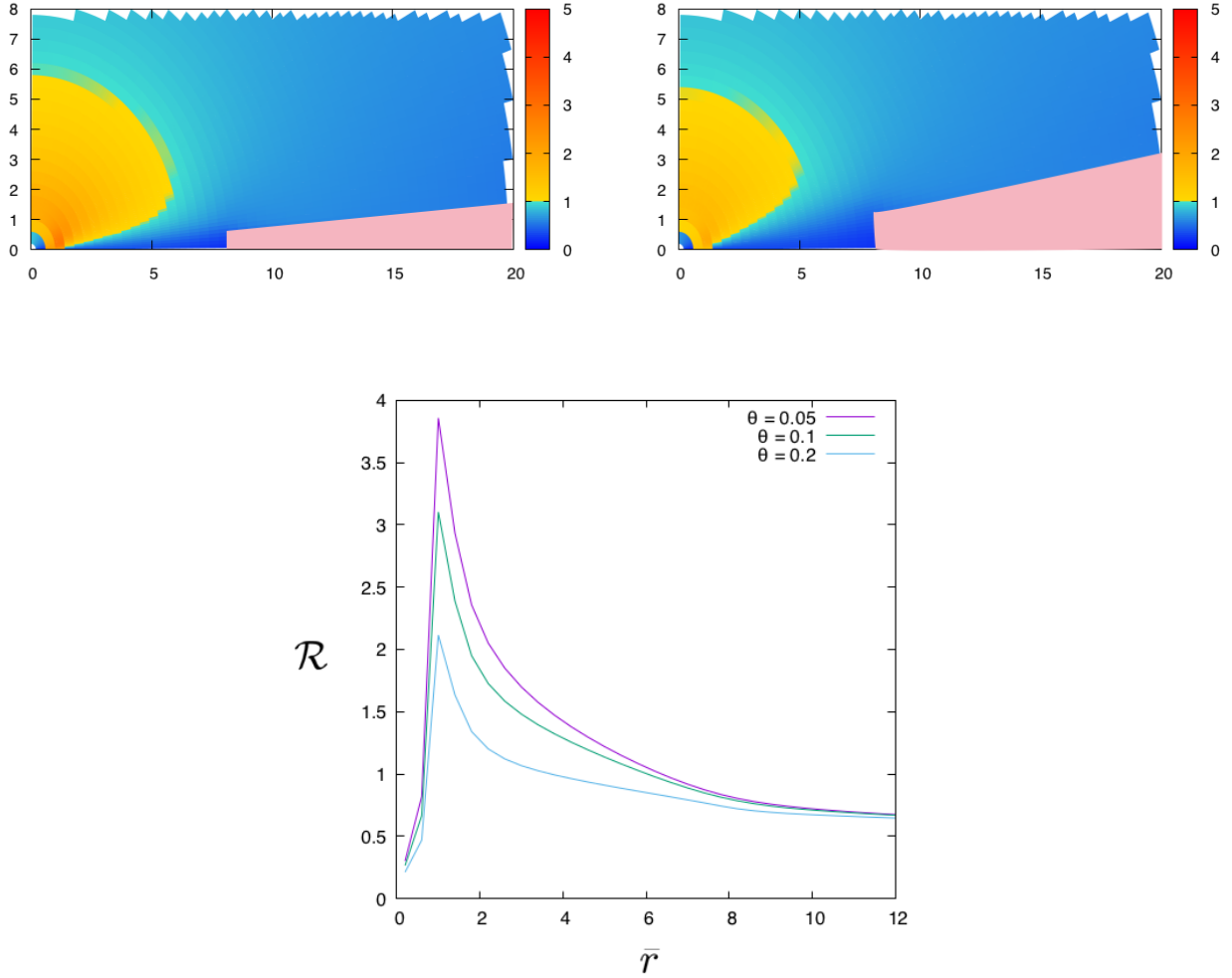


FIG. 5. \mathcal{R} for $\theta_0 = 0.1$ (top left) and $\theta_0 = 0.2$ (top right). \mathcal{R} along $\theta = 2\pi/5$ as a function of \bar{r} is also shown (bottom).

Appendix A: Scalar-field profile in Schwarzschild geometry

In the main text we have solved the Galileon field equation in the flat background. In order to see the scalar-field profile in the curved background, let us consider the covariant version of Eq. (2) in a *fixed* background:

$$\square\phi + \frac{c_3}{M^3} [(\square\phi)^2 - \nabla_\mu \nabla_\nu \phi \nabla^\mu \nabla^\nu \phi - R^{\mu\nu} \nabla_\mu \phi \nabla_\nu \phi] = \frac{\beta}{M_{\text{Pl}}} \rho, \quad (\text{A1})$$

where ∇_μ is the covariant derivative with respect to $g_{\mu\nu}$, $R_{\mu\nu}$ is the Ricci tensor, and we take

$$g_{\mu\nu} dx^\mu dx^\nu = - \left(1 - \frac{r_g}{r}\right) dt^2 + \left(1 - \frac{r_g}{r}\right)^{-1} dr^2 + r^2 d\Omega_2^2, \quad (\text{A2})$$

with $r_g = r_0$. We solve Eq.(A1) numerically for the matter configuration with $\bar{r}_1 = 8$, $\theta_0 = 0.05$, and $\mu = 36.8$. The resultant profile of ϕ should be compared with that in the flat background in Fig. 3. It can be seen that the profiles are not so different. We thus conclude that the effect of the background curvature does not change the result of anti-screening.

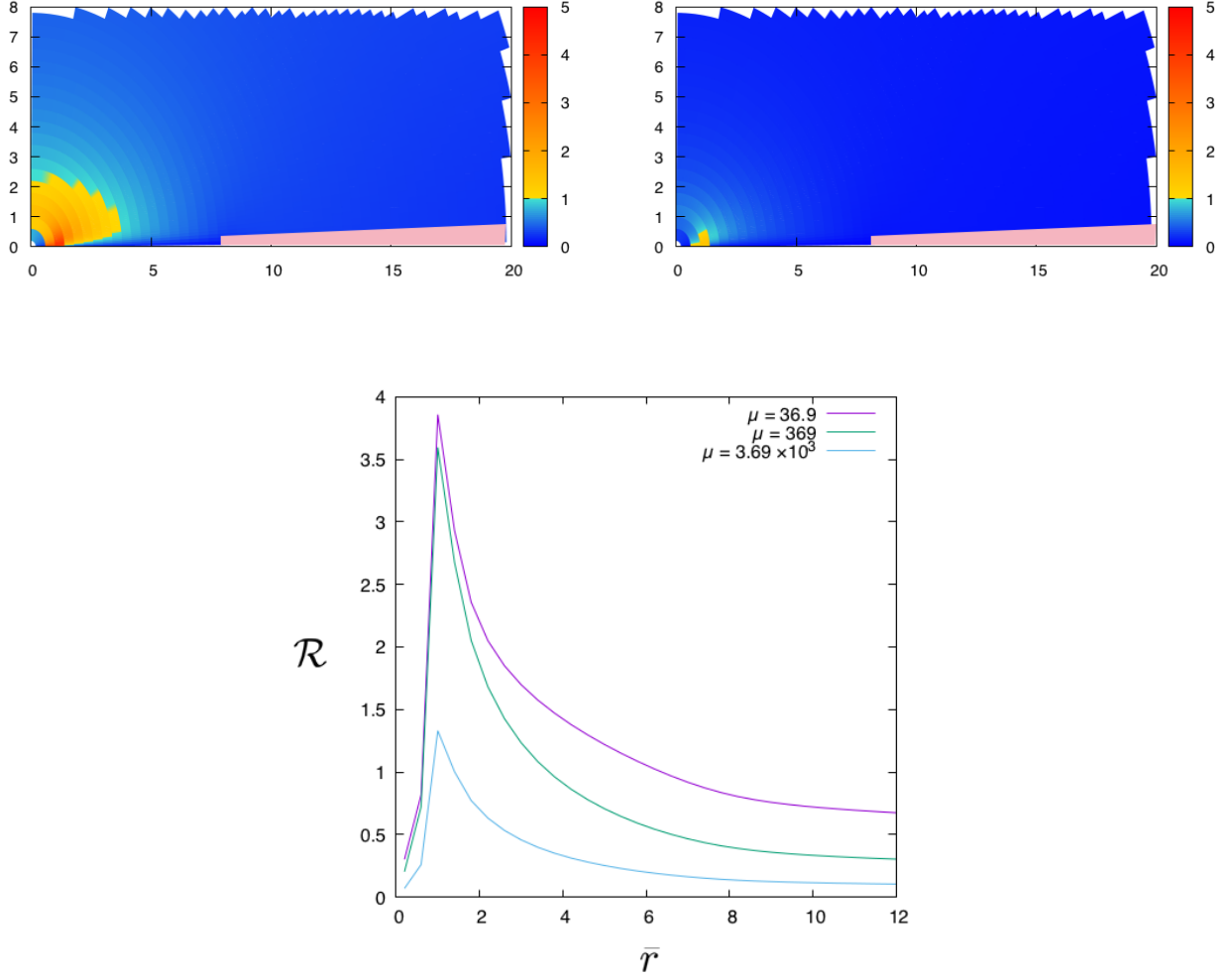


FIG. 6. \mathcal{R} for $\mu = 369$ (left) and $\mu = 3690$ (right). \mathcal{R} along $\theta = 2\pi/5$ as a function of \bar{r} is also shown (bottom).

Appendix B: Numerical scheme and convergence of results

Throughout this paper, we employed the numerical scheme developed in Ref. [34] to solve the field equation (2). Basically, we regard the non-linear terms of Eq. (2), the terms proportional to c_3 , as the extra source term such that

$$\Delta\phi = \frac{\beta}{M_{\text{Pl}}} \rho - \frac{c_3}{M^3} N[\phi]. \quad (\text{B1})$$

At the first step, we solve the linear equation with setting $N[\phi] = 0$ and obtain the solution ϕ_* . Then we update ϕ in the following manner:

$$\phi_{\text{new}}(r, \theta) = (1 - \omega)\phi_{\text{old}}(r, \theta) + \omega\phi_*(r, \theta), \quad (\text{B2})$$

with a mixing parameter $\omega = \mathcal{O}(0.01)$. At the next step, evaluating $N[\phi_{\text{new}}]$, we solve the field equation again, and ϕ is further updated. This iteration procedure is terminated when the update of ϕ is well suppressed, namely,

$$\frac{\|\phi_{\text{new}} - \phi_{\text{old}}\|}{\|\phi_{\text{new}}\|} < 10^{-8}, \quad (\text{B3})$$

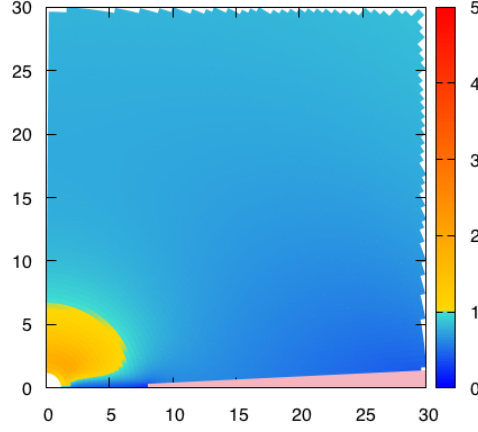


FIG. 7. \mathcal{R} in the Schwarzschild background. This should be compared with the left panel of Fig. 3.

where the norm $||\phi||$ is defined as $||\phi|| := \sqrt{\sum_{ij} \phi(r_i, \theta_j)^2}$. Note that, unless the parameter ω is small, this iteration scheme does not work since the non-linear term $N[\phi]$ induces quite a large change of the field configuration. For details, see Ref. [34].

The field equation solved in this paper, given in Eq. (2), is highly non-linear, and thus it should be confirmed whether our numerical results are reliable in the sense that they are well converged with the iteration scheme mentioned above. To see this, we solve the field equation with changing the number of grid points in the coordinate of (r, θ) , N_r and N_θ , and the position of the boundary in the radial direction, \bar{r}_{\max} . The fiducial values of N_r , N_θ and \bar{r}_{\max} in this paper are $N_r = 200$, $N_\theta = 100$ and $\bar{r}_{\max} = 80$. Note that we do not focus on the other numerical parameters since they control solely the convergence speed and the precision, and thus do not affect the final results.

Figure 8 shows \mathcal{R} evaluated at $\theta = 2\pi/5$. From the left panel, we find that our result is insensitive to the size of the computational box, which means that artificial effects from the boundary at $r = r_{\max}$ do not affect the feature at all. The remaining panels show the dependences of \mathcal{R} on the number of grids, N_r (center panel) and N_θ (right panel.) While the detailed structure of the peak around $\bar{r} \sim 1$ is sensitive to the spatial resolution, the fact that \mathcal{R} can be larger than the unity at $\bar{r} \lesssim 8$ is confirmed to be robust.

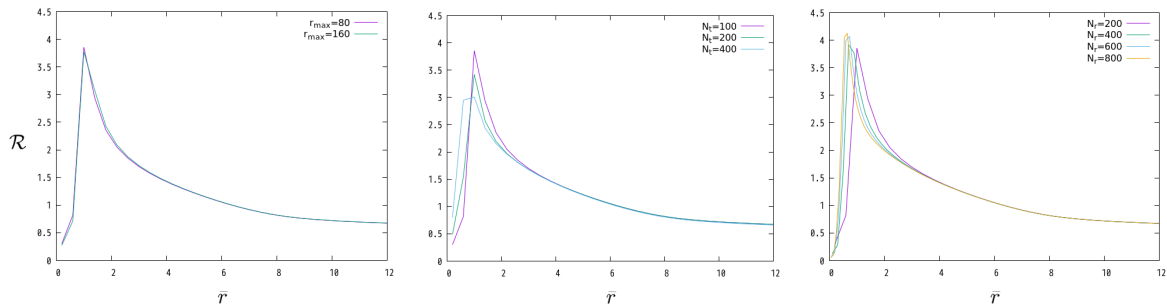


FIG. 8. The convergence check of numerical results; the dependence on \bar{r}_{\max} (left), on N_r (middle) and on N_θ (right).

-
- [1] S. Perlmutter *et al.* [Supernova Cosmology Project Collaboration], “Measurements of Omega and Lambda from 42 high redshift supernovae,” *Astrophys. J.* **517**, 565 (1999) [[astro-ph/9812133](#)].
 - [2] A. G. Riess *et al.* [Supernova Search Team], “Observational evidence from supernovae for an accelerating universe and a cosmological constant,” *Astron. J.* **116**, 1009 (1998) [[astro-ph/9805201](#)].

- [3] D. N. Spergel *et al.* [WMAP Collaboration], “First year Wilkinson Microwave Anisotropy Probe (WMAP) observations: Determination of cosmological parameters,” *Astrophys. J. Suppl.* **148**, 175 (2003) [[astro-ph/0302209](#)].
- [4] D. J. Eisenstein *et al.* [SDSS Collaboration], “Detection of the Baryon Acoustic Peak in the Large-Scale Correlation Function of SDSS Luminous Red Galaxies,” *Astrophys. J.* **633**, 560 (2005) [[astro-ph/0501171](#)].
- [5] K. N. Abazajian *et al.* [SDSS Collaboration], “The Seventh Data Release of the Sloan Digital Sky Survey,” *Astrophys. J. Suppl.* **182**, 543 (2009) [[arXiv:0812.0649](#) [astro-ph]].
- [6] P. A. R. Ade *et al.* [Planck Collaboration], “Planck 2013 results. XVI. Cosmological parameters,” *Astron. Astrophys.* **571**, A16 (2014) [[arXiv:1303.5076](#) [astro-ph.CO]].
- [7] See, *e.g.*, E. J. Copeland, M. Sami and S. Tsujikawa, “Dynamics of dark energy,” *Int. J. Mod. Phys. D* **15**, 1753 (2006), [[hep-th/0603057](#)].
- [8] See, *e.g.*, T. Clifton, P. G. Ferreira, A. Padilla and C. Skordis, “Modified gravity and cosmology,” *Phys. Rep.*, **513**, 1 (2012), [[arXiv:1106.2476](#) [astro-ph.CO]].
- [9] C. M. Will, “The Confrontation between General Relativity and Experiment,” *Living Rev. Rel.* **17**, 4 (2014) [[arXiv:1403.7377](#) [gr-qc]].
- [10] B. Bertotti, L. Iess and P. Tortora, “A test of general relativity using radio links with the Cassini spacecraft,” *Nature* **425**, 374 (2003).
- [11] J. Khoury and A. Weltman, “Chameleon cosmology,” *Phys. Rev. D* **69**, 044026 (2004) [[astro-ph/0309411](#)].
- [12] K. Hinterbichler and J. Khoury, “Symmetron Fields: Screening Long-Range Forces Through Local Symmetry Restoration,” *Phys. Rev. Lett.* **104**, 231301 (2010) [[arXiv:1001.4525](#) [hep-th]].
- [13] P. Brax, C. van de Bruck, A. C. Davis and D. Shaw, “The Dilaton and Modified Gravity,” *Phys. Rev. D* **82**, 063519 (2010) [[arXiv:1005.3735](#) [astro-ph.CO]].
- [14] C. Burrage and J. Khoury, “Screening of scalar fields in Dirac-Born-Infeld theory,” *Phys. Rev. D* **90**, no. 2, 024001 (2014) [[arXiv:1403.6120](#) [hep-th]].
- [15] E. Babichev, C. Deffayet and R. Ziour, “k-Mouflage gravity,” *Int. J. Mod. Phys. D* **18**, 2147 (2009) [[arXiv:0905.2943](#) [hep-th]].
- [16] P. Brax, C. Burrage and A. C. Davis, “Screening fifth forces in k-essence and DBI models,” *JCAP* **1301**, 020 (2013) [[arXiv:1209.1293](#) [hep-th]].
- [17] A. Nicolis, R. Rattazzi and E. Trincherini, “The Galileon as a local modification of gravity,” *Phys. Rev. D* **79**, 064036 (2009) [[arXiv:0811.2197](#) [hep-th]].
- [18] C. Deffayet, G. Esposito-Farese and A. Vikman, “Covariant Galileon,” *Phys. Rev. D* **79**, 084003 (2009) [[arXiv:0901.1314](#) [hep-th]].
- [19] C. Deffayet, S. Deser and G. Esposito-Farese, “Generalized Galileons: All scalar models whose curved background extensions maintain second-order field equations and stress-tensors,” *Phys. Rev. D* **80**, 064015 (2009) [[arXiv:0906.1967](#) [gr-qc]].
- [20] A. I. Vainshtein, “To the problem of nonvanishing gravitation mass,” *Phys. Lett.* **39B**, 393 (1972).
- [21] E. Babichev and C. Deffayet, “An introduction to the Vainshtein mechanism,” *Class. Quant. Grav.* **30**, 184001 (2013) [[arXiv:1304.7240](#) [gr-qc]].
- [22] R. Kimura, T. Kobayashi and K. Yamamoto, “Vainshtein screening in a cosmological background in the most general second-order scalar-tensor theory,” *Phys. Rev. D* **85**, 024023 (2012) [[arXiv:1111.6749](#) [astro-ph.CO]].
- [23] T. Narikawa, T. Kobayashi, D. Yamauchi and R. Saito, “Testing general scalar-tensor gravity and massive gravity with cluster lensing,” *Phys. Rev. D* **87**, 124006 (2013) [[arXiv:1302.2311](#) [astro-ph.CO]].
- [24] K. Koyama, G. Niz and G. Tasinato, “Effective theory for the Vainshtein mechanism from the Horndeski action,” *Phys. Rev. D* **88**, 021502 (2013) [[arXiv:1305.0279](#) [hep-th]].
- [25] R. Kase and S. Tsujikawa, “Screening the fifth force in the Horndeski’s most general scalar-tensor theories,” *JCAP* **1308**, 054 (2013) [[arXiv:1306.6401](#) [gr-qc]].
- [26] G. W. Horndeski, “Second-order scalar-tensor field equations in a four-dimensional space,” *Int. J. Theor. Phys.* **10**, 363 (1974).
- [27] C. Deffayet, X. Gao, D. A. Steer and G. Zahariade, “From k-essence to generalised Galileons,” *Phys. Rev. D* **84**, 064039 (2011) [[arXiv:1103.3260](#) [hep-th]].
- [28] T. Kobayashi, M. Yamaguchi and J. Yokoyama, “Generalized G-inflation: Inflation with the most general second-order field equations,” *Prog. Theor. Phys.* **126**, 511 (2011) [[arXiv:1105.5723](#) [hep-th]].
- [29] T. Kobayashi, Y. Watanabe and D. Yamauchi, “Breaking of Vainshtein screening in scalar-tensor theories beyond Horndeski,” *Phys. Rev. D* **91**, no. 6, 064013 (2015) [[arXiv:1411.4130](#) [gr-qc]].
- [30] M. Crisostomi and K. Koyama, “Vainshtein mechanism after GW170817,” *Phys. Rev. D* **97**, no. 2, 021301 (2018) [[arXiv:1711.06661](#) [astro-ph.CO]].
- [31] D. Langlois, R. Saito, D. Yamauchi and K. Noui, “Scalar-tensor theories and modified gravity in the wake of GW170817,” [arXiv:1711.07403](#) [gr-qc].
- [32] A. Dima and F. Vernizzi, “Vainshtein Screening in Scalar-Tensor Theories before and after GW170817: Constraints on Theories beyond Horndeski,” [arXiv:1712.04731](#) [gr-qc].
- [33] J. K. Bloomfield, C. Burrage and A. C. Davis, “Shape dependence of Vainshtein screening,” *Phys. Rev. D* **91**, no. 8, 083510 (2015) [[arXiv:1408.4759](#) [gr-qc]].
- [34] T. Hiramatsu, W. Hu, K. Koyama and F. Schmidt, “Equivalence Principle Violation in Vainshtein Screened Two-Body Systems,” *Phys. Rev. D* **87**, no. 6, 063525 (2013) [[arXiv:1209.3364](#) [hep-th]].
- [35] J. Chagoya, K. Koyama, G. Niz and G. Tasinato, “Galileons and strong gravity,” *JCAP* **1410**, no. 10, 055 (2014) [[arXiv:1407.7744](#) [hep-th]].

- [36] C. de Rham, A. Matas and A. J. Tolley, “Galileon Radiation from Binary Systems,” *Phys. Rev. D* **87**, no. 6, 064024 (2013) [[arXiv:1212.5212](#) [hep-th]].
- [37] C. Burrage, E. J. Copeland, A. Moss and J. A. Stevenson, “The shape dependence of chameleon screening,” [arXiv:1711.02065](#) [astro-ph.CO].
- [38] A. C. Davis, R. Gregory, R. Jha and J. Muir, “Astrophysical black holes in screened modified gravity,” *JCAP* **1408**, 033 (2014) [[arXiv:1402.4737](#) [astro-ph.CO]].
- [39] A. C. Davis, R. Gregory and R. Jha, “Black hole accretion discs and screened scalar hair,” *JCAP* **1610**, no. 10, 024 (2016) [[arXiv:1607.08607](#) [gr-qc]].